

A cyclic voltammetric study of the kinetics and mechanism of electrodeposition of manganese dioxide

SHALINI RODRIGUES*, N. MUNICHANDRAIAH† and A. K. SHUKLA*

Solid State and Structural Chemistry Unit and Department of Inorganic and Physical Chemistry†, Indian Institute of Science, Bangalore – 560 012, India*

Received 1 December 1997; revised 24 March 1998

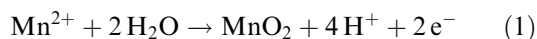
The kinetics and mechanism of electrooxidation of Mn^{2+} ions to MnO_2 (EMD) has been studied in electrolytes comprising MnSO_4 and H_2SO_4 by cyclic voltammetry at 80 °C. The voltammogram of a Pt electrode cycled between 0.6 and 1.6 V vs SCE exhibits an anodic current peak at about 1.3 V vs SCE resulting in the deposition of MnO_2 on the electrode, while a cathodic peak appears at 0.8 V vs SCE. It is shown that the pair of peaks do not correspond to a single reversible reaction but represent two separate irreversible electrode processes. The cyclic voltammetric peak current for the deposition of EMD is found to be proportional to the square root of Mn^{2+} ion concentration in the electrolyte and independent of acid concentration. Based on these results, a mechanism for the formation of EMD involving diffusion of Mn^{2+} ions to the electrode surface, oxidation of $\text{Mn}_{\text{surface}}^{2+}$ to $\text{Mn}_{\text{ads}}^{3+}$, and H_2O to OH_{ads} as the primary oxidation steps is invoked. $\text{Mn}_{\text{ads}}^{3+}$ ions dissociate disproportionately into $\text{Mn}_{\text{ads}}^{2+}$ and $\text{Mn}_{\text{ads}}^{4+}$ ions at the electrode surface. The $\text{Mn}_{\text{ads}}^{2+}$ and $\text{Mn}_{\text{ads}}^{4+}$ ions, respectively, react with OH_{ads} and H_2O resulting in the formation of EMD.

Keywords: *manganese dioxide, electrodeposition, cyclic voltammetry, multistep mechanism, disproportionate dissociation*

1. Introduction

Manganese dioxides are the most utilized frameworks for battery cathodes. Manganese dioxides are broadly categorized into three groups namely natural manganese dioxide (NMD), chemical manganese dioxide (CMD), and electrochemical manganese dioxide (EMD). Among them, EMD exhibits the greatest battery activity for most applications. EMD is usually γ - MnO_2 .

The electrochemical deposition of EMD on an inert electrode in an electrolyte containing Mn^{2+} ions occurs following the reaction:



It is reported [1] that the mechanism of MnO_2 deposition is represented by Reaction 1. However, it is unlikely that this reaction occurs in a single step for the following reasons: (i) the oxidation state of manganese increases from 2+ to 4+, and it is improbable that the two electrons are transferred in a single step, and (ii) for the formation of MnO_2 , oxidation of water molecule must occur concomitantly with the oxidation of Mn^{2+} . Therefore, it is most probable that the overall Reaction 1 occurs in a sequence of simple reaction steps. In the present communication, the kinetics and mechanism of Reaction 1 are reported as investigated by cyclic voltammetry.

2. Experimental details

Solutions were prepared in doubly distilled water using AR grade chemicals. Cyclic voltammetric experiments were conducted in a three electrode cell containing a Pt working electrode (area 0.4 cm²) which was symmetrically placed between two other Pt counter electrodes. A saturated calomel electrode (SCE) was used as the reference electrode. The cell temperature was maintained at the required temperature within ± 1 °C by thermostating. For characterization of EMD samples, thick layers of MnO_2 were galvanostatically deposited on Ti, platinized Ti or Pb anodes in a similar cell at a current density of 1.5 mA cm⁻² or potentiostatically at 1.35 V vs SCE. The deposited EMD was mechanically removed, powdered and the XRD patterns recorded on a Rich-Siefert XRD 3000 TT X-ray diffractometer.

Cyclic voltammograms were recorded using a EG&G PARC Versastat driven by an IBM compatible computer and EG&G PARC electrochemistry software (model M270). For galvanostatic experiments, a regulated d.c. power source was employed in series with a high resistance and an ammeter. A Gerhard Bank potentiostat (model MP75) was used for potentiostatic deposition of MnO_2 .

3. Results and discussion

The XRD pattern of the EMD sample prepared in the present study is found to be poorly crystalline

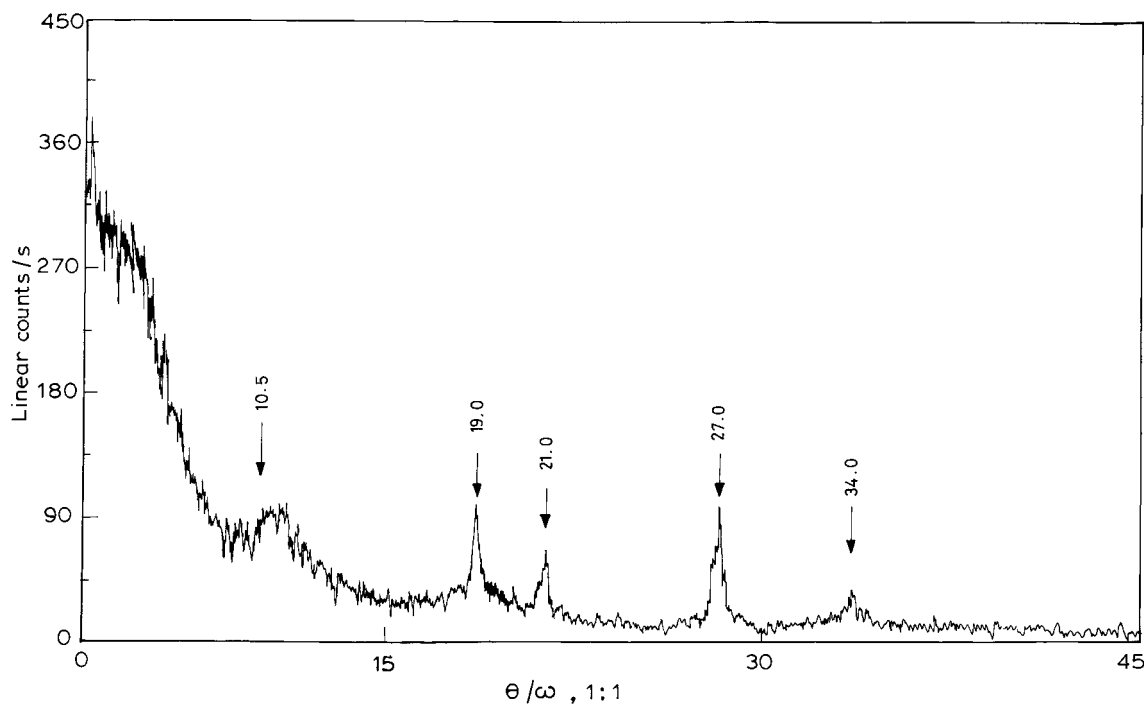


Fig. 1. Powder XRD pattern of electrolytic manganese dioxide.

(Fig. 1). The poorly crystalline nature of EMD is described in the literature [2-4]. It is reported [4] that the X-ray powder diffraction patterns of EMD are always of rather poor quality and consist at best of a small number of sharp and broad lines on top of a diffused background. Although the structure is not

directly amenable by conventional diffraction techniques, the EMD is generally regarded as γ - MnO_2 .

The cyclic voltammograms recorded at several scan rates in a typical solution comprising 0.5 M MnSO_4 + 0.4 M H_2SO_4 at a Pt electrode at 80 °C are shown in Fig. 2. In all these voltammograms, the

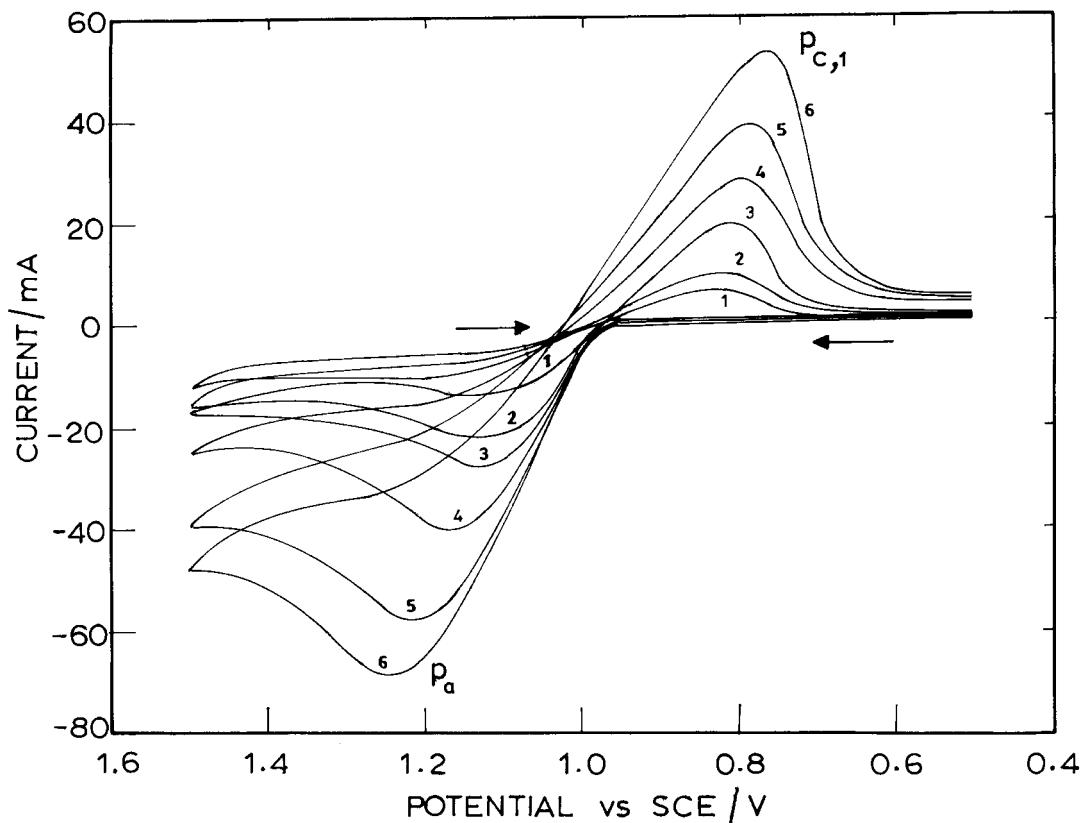


Fig. 2. Cyclic voltammograms in 0.5 M MnSO_4 + 0.4 M H_2SO_4 electrolyte on a Pt electrode (area 0.4 cm^2) at 80 °C at a scan rate of (1) 5, (2) 10, (3) 20, (4) 50, (5) 100 and (6) 200 mV s^{-1} . Anodic current is denoted by a negative sign. Potential scan was initiated at 0.5 V vs SCE and scan direction was reversed at 1.5 V vs SCE.

anodic current peak (p_a) lies between 1.15 and 1.3 V vs SCE and may be ascribed to the oxidation of Mn^{2+} ions to MnO_2 as shown in Reaction 1. A shift of 0.13 V in peak potential accompanied by a drift of 54.3 mA in peak current is observed when the scan rate is changed from 5 to 200 $mV s^{-1}$. As the electrode reached the potential region of this anodic peak, the surface of the Pt electrode turned black due to the deposition of MnO_2 . It was observed that at potentials beyond 1.5 V vs SCE, oxygen evolution reaction (OER) commenced. Oxidation of MnO_2 to higher valence oxides such as MnO_4^- ions is also possible at such highly positive potentials. However, no current peak corresponding to this reaction appeared on the voltammograms. On reversing the direction of the potential sweep at 1.5 V, a cathodic current peak ($p_{c,1}$) appeared at about 0.775 V vs SCE (Fig. 2). The following reactions are possible around this potential to account for peak $p_{c,1}$: (i) the reduction of MnO_2 , (ii) the reduction of intermediate species of manganese, such as Mn^{3+} ions to Mn^{2+} ions; Mn^{3+} ions could have been formed by oxidation of Mn^{2+} ions during the anodic cycle, and (iii) the reduction of adsorbed oxygen or oxygen containing species such as OH_{ads} that may be formed on the electrode surface during the anodic cycle.

To assign the cathodic peak ($p_{c,1}$) to one of the above possible reactions, the following experiments were carried out. The voltammograms were recorded by holding the electrode at the switching potential

(1.5 V vs SCE) for several minutes before reversing the potential sweep. It was expected that the intermediate species (e.g., Mn^{3+} ions) could be oxidized to MnO_2 during the holding time and therefore would not be available at the electrode surface for reduction during the reverse scan. It was found that the cathodic peak current ($I_{p_{c,1}}$) remained the same for all holding times. These results suggested that the appearance of the cathodic peak was not due to the reduction of the intermediate species. In another set of experiments, the voltammograms were recorded by reversing the potential sweep at different potentials between 1.2 and 1.6 V vs SCE. Around 1.2 V vs SCE, oxygen evolution did not start and around 1.6 V vs SCE, oxygen evolution proceeded vigorously as indicated by the gas evolution at the electrode surface and also from the increase in current on the voltammograms. If adsorbed oxygen species undergo reduction resulting in the appearance of peak ($p_{c,1}$), the peak current would increase with increase in switching potentials [5]. The voltammograms recorded for different switching potentials showed that the peak current $I_{p_{c,1}}$ remained unaltered for all the curves, suggesting that reduction of oxygen species was not responsible for the presence of cathodic peak ($p_{c,1}$). It is interesting to note that when the switching potentials were chosen in the potential region between 1.6 and 2 V vs SCE, the cathodic peak current $I_{p_{c,1}}$ decreased with increase of switching potential, as shown in Fig. 3. This can be attributed to the oxidation of

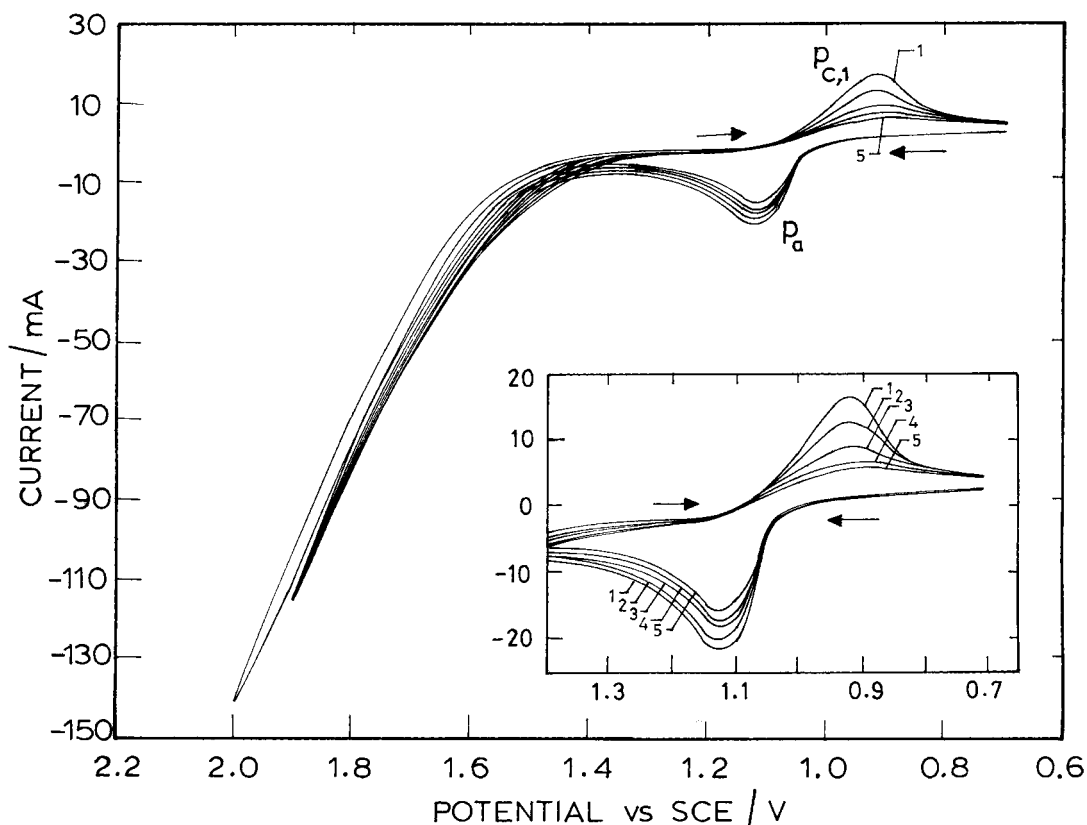


Fig. 3. Cyclic voltammograms in 0.5 M $MnSO_4$ + 1 M H_2SO_4 electrolyte on a Pt electrode (area 0.4 cm^2) at 80 $^{\circ}C$ between the initial potential 0.7 V vs SCE and switching potential, (1) 1.6, (2) 1.7, (3) 1.8, (4) 1.9 and (5) 2 V vs SCE at 50 $mV s^{-1}$ scan rate. Current peak region is expanded and shown in insert.

MnO₂ to soluble MnO₄⁻ ions, along with oxygen evolution leading to thinner deposits of MnO₂ at such highly positive potentials. Accordingly, a reduction in peak current $I_{pc,1}$ is seen. These results, suggest that the cathodic peak ($p_{c,1}$) may be assigned to MnO₂ reduction.

To examine whether the anodic peak (p_a) and cathodic peak ($p_{c,1}$) correspond to a reversible reaction, voltammograms were recorded at different scan rates (v). The peak currents are plotted against $v^{1/2}$ in Fig. 4. It is found that both I_{pa} and $I_{pc,1}$ increase linearly with $v^{1/2}$, suggesting that the reactions corresponding to both these peaks are diffusion controlled. If the peaks correspond to a reversible reaction, the cathodic and anodic peak potentials should be separated by about 30 mV and the peak potentials should be independent of the scan rate. It is found that the anodic and cathodic peak potentials are separated by several hundred millivolts (see Fig. 2) and the peak potentials change with scan rate (Fig. 5). Furthermore, the charge associated with the cathodic peak ($p_{c,1}$) is lesser than that of the anodic peak (p_a) at any scan rate. Also, the black deposit of MnO₂ was found to be present on the platinum electrode even after $p_{c,1}$ appeared. These facts imply that the current peaks p_a and $p_{c,1}$ do not represent a reversible reaction. On extending the voltammogram to 0 V vs SCE (Fig. 6), an additional cathodic peak ($p_{c,2}$) appears at a potential more negative to the peak potential of $p_{c,1}$ and becomes more pronounced at higher scan rates.

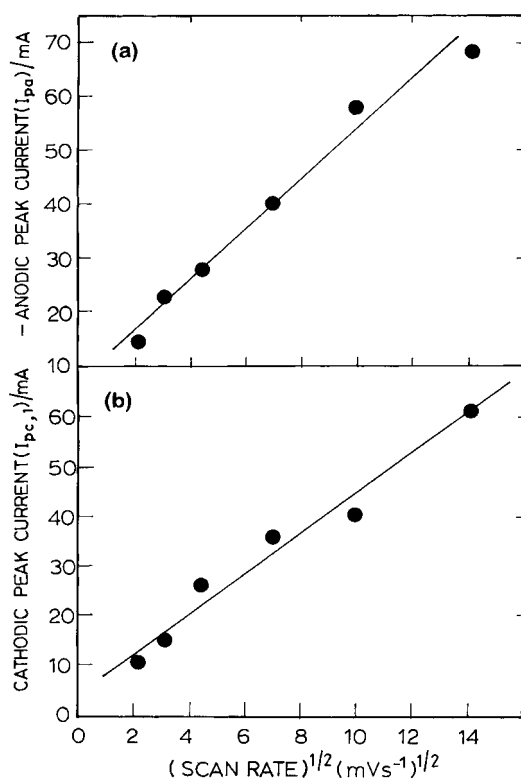


Fig. 4. (a) Anodic peak current (I_{pa}) and (b) cathodic peak current ($I_{pc,1}$) as a function of square root of scan rate (v). The voltammograms were recorded in 0.5 M MnSO₄ + 0.4 M H₂SO₄ electrolyte on a Pt electrode (area 0.4 cm²) at 80 °C.

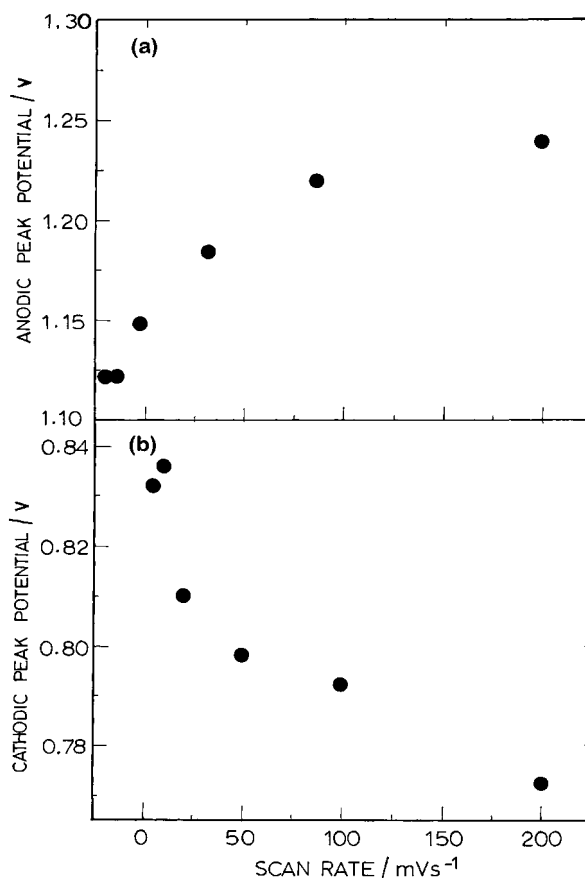
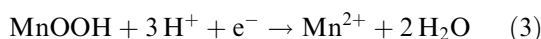
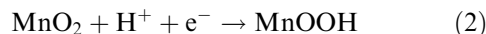


Fig. 5. (a) Anodic peak potential (E_{pa} vs SCE) and (b) cathodic peak potential ($E_{pc,1}$ vs SCE) as a function of scan rate (v). The voltammograms were recorded in 0.5 M MnSO₄ + 0.4 M H₂SO₄ electrolyte on a Pt electrode (area 0.4 cm²) at 80 °C.

Lee, Maskell and Tye [6] also have reported two cathodic current peaks in their voltammograms of MnO₂ in dilute H₂SO₄. These authors found a variation in the second peak potential with the substrate material. Maskell [7] has invoked a metal/semiconductor interface model to explain these results. In the present study, however, the electrodeposited layer of MnO₂ was substantially thick. Furthermore, the layer of MnO₂ deposited during the anodic half cycle was not completely reduced during the cathodic half cycle consisting of both $p_{c,1}$ and $p_{c,2}$ peaks. This was evident when the Pt electrode was found black at the end of the potential cycle. It may, therefore, be conjectured that the reduction of MnO₂ does not occur in a single step, but in two steps. The following scheme for such a reduction is thus envisaged:



The cathodic peak $p_{c,1}$ is attributed to Reaction 2 and the peak $p_{c,2}$ to Reaction 3.

For the overall reaction leading to the formation of MnO₂ from Mn²⁺ ions by anodic oxidation as represented by Reaction 1, it is evident that the concentrations of Mn²⁺ ions and H⁺ ions in the electrolyte and temperature influence the kinetics of the reaction. The cyclic voltammetric peak current of a simple irreversible electron transfer reaction is

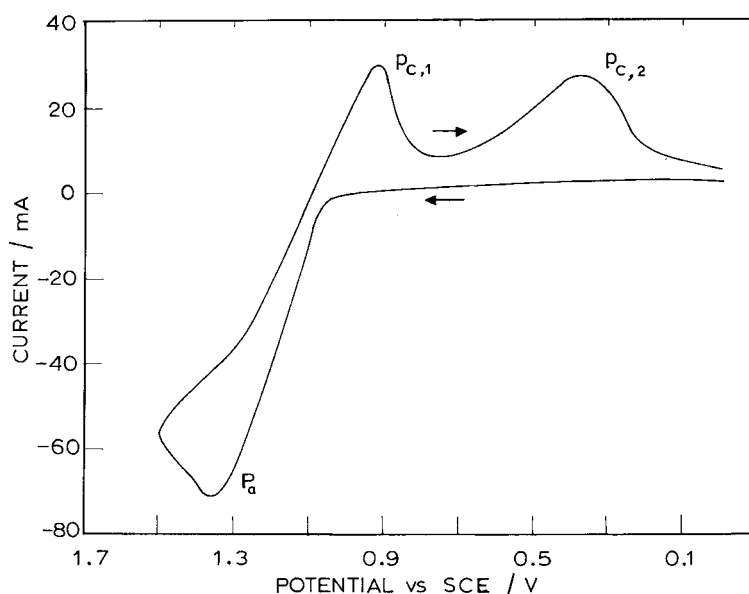


Fig. 6. Cyclic voltammograms recorded between 0.0 and 1.6 V vs SCE at 200 mV s^{-1} scan rate in $0.5 \text{ M MnSO}_4 + 0.4 \text{ M H}_2\text{SO}_4$ electrolyte on a Pt electrode (area 0.4 cm^2) at 80°C .

proportional to the concentration (C) of the reactant [8] and is given as

$$I_p = kn(\alpha_c n_\alpha)^{1/2} CD^{1/2} \nu^{1/2} \quad (4)$$

where n is the total number of electrons involved in the overall reaction, n_α is the number of electrons transferred up to the rate determining step, D is diffusion coefficient and k is a constant. Normally, $d \ln I_p / d \ln C$ should be unity for a simple diffusion-controlled reaction. Cyclic voltammograms were recorded in several electrolyte solutions of different concentrations of MnSO_4 and H_2SO_4 . The variation of peak current (I_{pa}) with H_2SO_4 concentration is shown in Fig. 7. It is seen that the peak current remains almost unaltered at all concentrations of H_2SO_4 . This is in accordance with Reaction 1 in

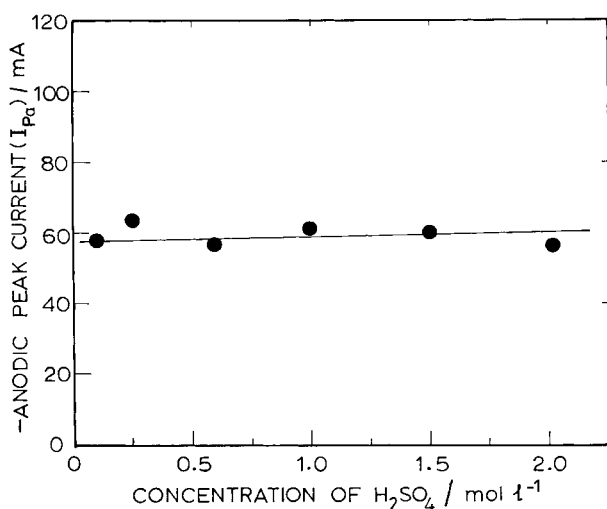
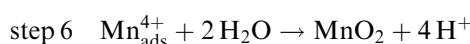
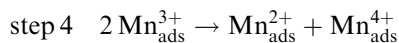
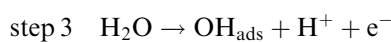
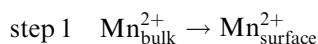


Fig. 7. The anodic peak current (I_{pa}) at 200 mV s^{-1} scan rate as a function of H_2SO_4 concentration while MnSO_4 concentration was maintained constant at 0.5 mol dm^{-3} . Voltammograms were recorded on a Pt electrode (area 0.4 cm^2) at 80°C .

which the H^+ ions are present as the product and the reaction is irreversible as discussed above.

The variation of peak current (I_{pa}) with the concentration of Mn^{2+} ions is shown in Fig. 8. The variation is non-linear, although it is expected to be linear in accordance with Equation 4 for a simple electron transfer reaction. A logarithmic plot of the same data, however, is found to be linear as shown in Fig. 9. The slope obtained for all scan rates is nearly constant, at 0.50 ± 0.02 . This means that the anodic peak current (I_{pa}) is proportional to the square root of Mn^{2+} ion concentration and therefore suggests that the anodic deposition of MnO_2 involves a complex mechanism. Furthermore, an examination of Reaction 1 suggests that Mn^{2+} ions oxidize to Mn^{4+} with simultaneous oxidation of H_2O molecules. The two-electron transfer process involving oxidation of Mn^{2+} to Mn^{4+} , accompanied by the oxidation of H_2O cannot occur in a single step. Hence, the following multistep mechanism is envisaged for the anodic deposition of MnO_2 :



The potential sweep experiments were carried out in unstirred electrolytes and current peaks appeared, as discussed above, during forward and reverse potential scans. Therefore, it is considered that diffusion process is the rate determining step (Fig. 4). Accordingly, diffusion of Mn^{2+} ion from bulk to the electrode surface is shown in step 1 above. Oxidation of Mn^{2+} at the electrode surface to $\text{Mn}_{\text{ads}}^{3+}$ is the most

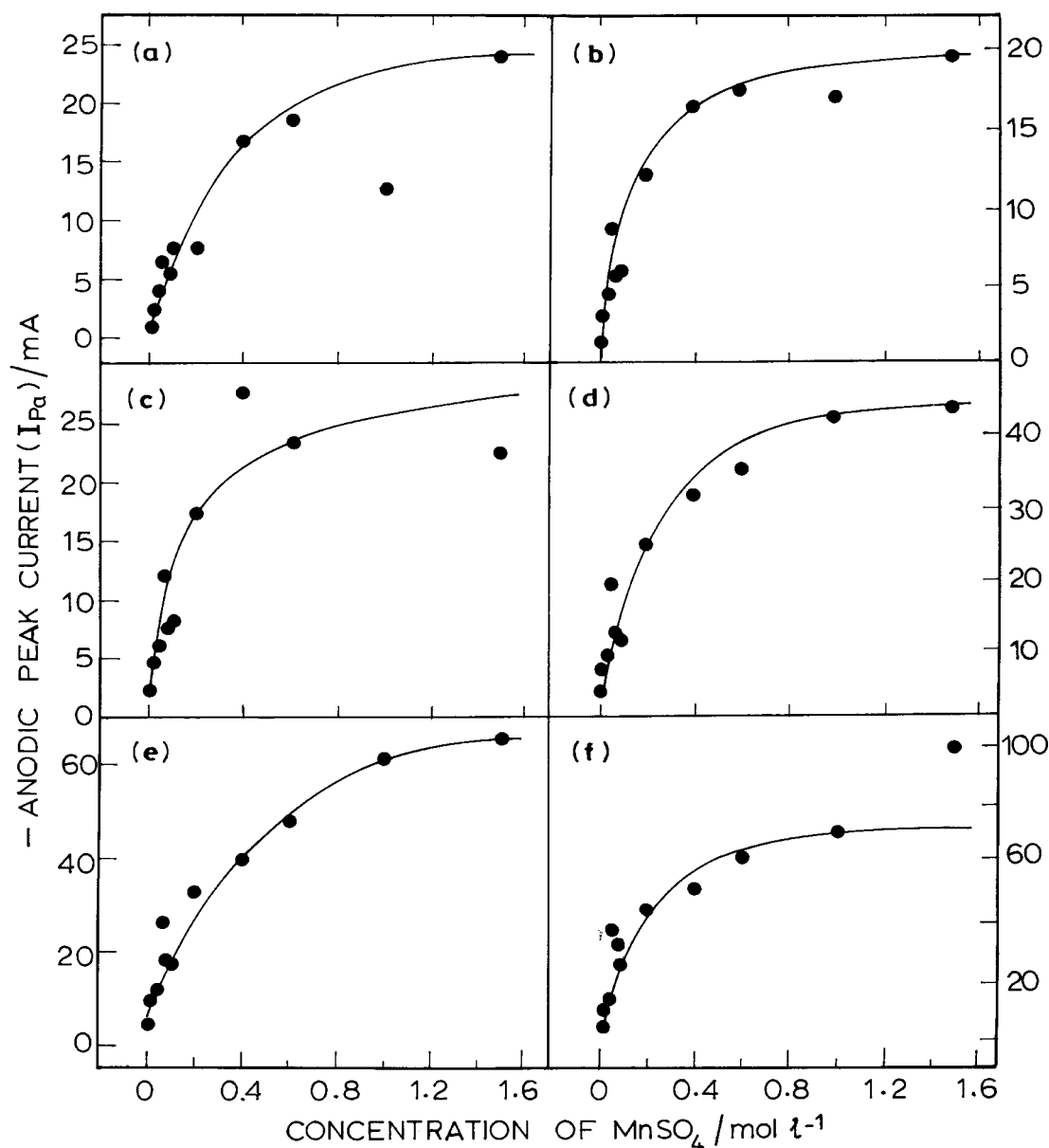


Fig. 8. The anodic peak current (I_{pa}) as a function of $MnSO_4$ concentration while H_2SO_4 concentration was maintained constant at 0.5 mol dm^{-3} . Voltammograms were recorded at a scan rate of (a) 5, (b) 10, (c) 20, (d) 50, (e) 100 and (f) 200 mV s^{-1} on a Pt electrode (area 0.4 cm^2) at 80°C .

probable single electron transfer step, which is shown in step 2. In the step 3 above, oxidation of H_2O is considered as another single electron transfer process, producing adsorbed OH radicals. There is an ambiguity in the literature [9] on the formation of Mn_{ads}^{3+} and its subsequent decomposition as shown in step 4. The standard potential for Mn^{2+}/Mn^{3+} couple is 1.5 V vs NHE. The deposition of MnO_2 occurs at a potential, which is negative to 1.5 V vs NHE. On this basis, it has been assumed by various investigators [1] that the formation of Mn^{3+} is not possible in the mechanism. However, various *in situ* spectroelectrochemical studies have confirmed the formation of Mn^{3+} ions before the deposition of MnO_2 [10]. This has led to a conclusion that the published standard potential of 1.5 V (vs NHE) for Mn^{2+}/Mn^{3+} is probably higher [9]. In the mechanism, steps 2 and 3

are only the electron-transfer reactions each involving a single electron. Mn_{ads}^{3+} ions formed in the step 2 are unstable [11] and are shown to dissociate into Mn^{2+} and Mn^{4+} ions in the adsorbed state in step 4. This type of disproportionate decomposition has also been reported in the literature [12]. The interesting aspect of step 4 is the reformation of the bulk reactant (i.e., Mn^{2+} ion) at the electrode surface in the adsorbed state, which can further undergo oxidation to Mn^{3+} according to step 2. It appears that the regeneration of Mn^{2+} at the electrode surface (step 4) and its subsequent oxidation to Mn^{3+} (step 2) reflect the square root dependence of concentration on peak current as discussed above (Fig. 9). An additional possibility of Mn_{ads}^{2+} undergoing chemical oxidation and combining with OH_{ads} (formed in step 3) resulting in MnO_2 is shown in step 5. Mn_{ads}^{4+} ions

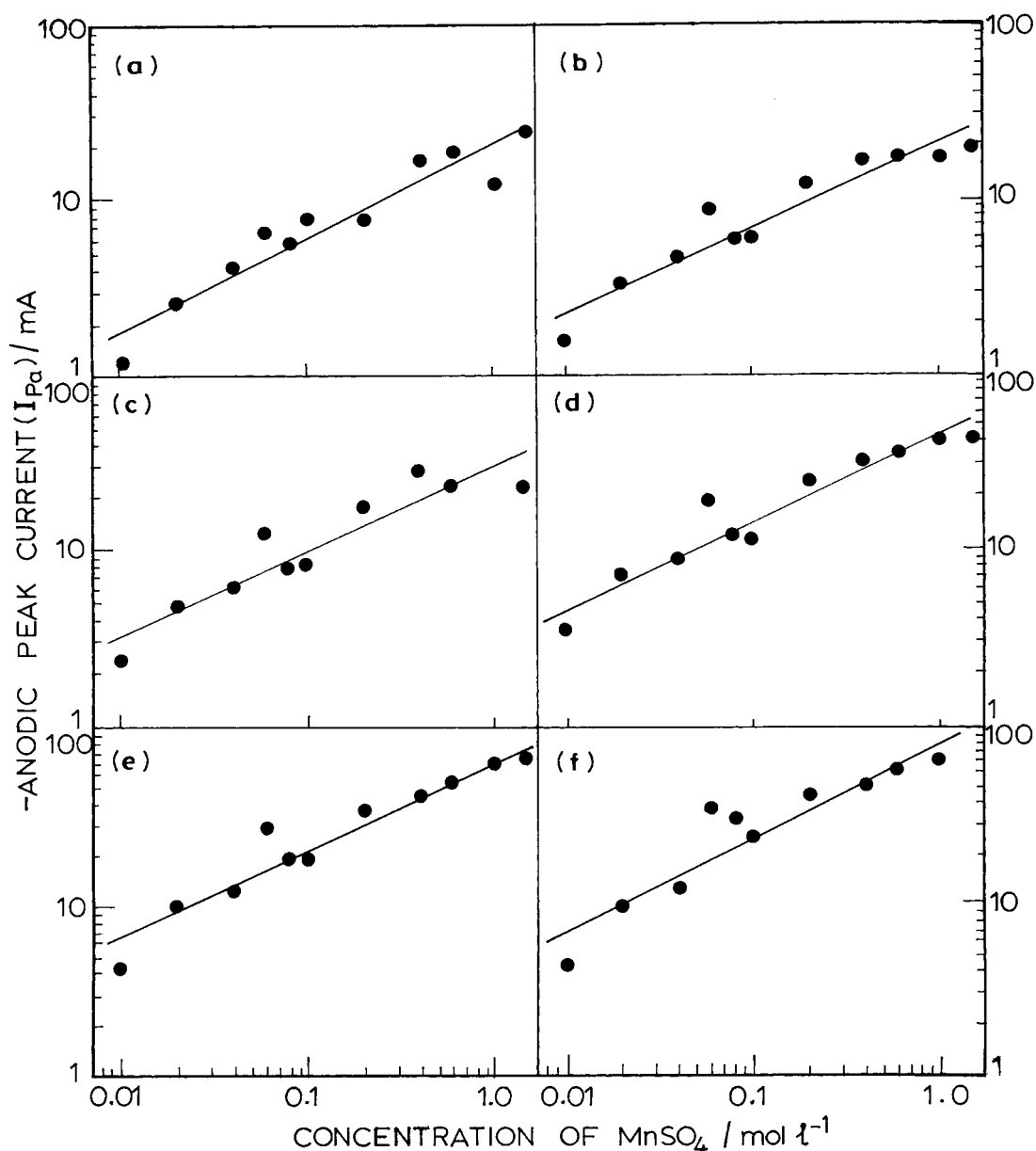


Fig. 9. The data of Fig. 8 on logarithmic scales.

formed in step 4 combine with H_2O in a chemical step (step 6) leading to the formation of MnO_2 on the electrode surface.

4. Conclusions

A scheme is proposed for the anodic deposition of electrolytic manganese dioxide based on cyclic voltammetric data. It involves diffusion of Mn^{2+} ions to the electrode surface, the oxidation of $\text{Mn}_{\text{surface}}^{2+}$ to $\text{Mn}_{\text{ads}}^{3+}$ and the oxidation of H_2O to OH_{ads} . $\text{Mn}_{\text{ads}}^{3+}$ ions dissociate disproportionately into $\text{Mn}_{\text{ads}}^{2+}$ and $\text{Mn}_{\text{ads}}^{4+}$ ions at the electrode surface. These $\text{Mn}_{\text{ads}}^{2+}$ and $\text{Mn}_{\text{ads}}^{4+}$ ions react with OH_{ads} and H_2O , respectively, in chemical steps leading to the formation of MnO_2 .

References

- [1] A. Kozawa, in 'Batteries Vol. 1 Manganese Dioxide' edited by K. V. Kordesch (Marcel Dekker, New York, 1974), p. 385.
- [2] K. Matsuki, T. Endo and H. Kamada, *Electrochim. Acta* **29** (1984) 983.
- [3] A. K. Sleight, J. J. Murray and W. R. McKinnor, *ibid.* **36** (1991) 1469.
- [4] Y. Chabre and J. Pannetier, *Prog. Solid State Chem.* **23** (1995) 1.
- [5] N. Munichandraiah, *J. Electroanal. Chem.* **309** (1991) 199.
- [6] J. A. Lee, W. C. Maskell and F. L. Tye, *J. Electroanal. Chem.* **79** (1997) 79.
- [7] W. C. Maskell, *J. Electroanal. Chem.* **198** (1985) 127.
- [8] R. Greef, R. Peat, L. M. Peter, D. Pletcher and J. Robinson in 'Instrumental methods in electrochemistry' (Ellis Horwood, 1995), p. 186.
- [9] T. N. Anderson, in 'Modern Aspects of Electrochemistry No. 30' edited by R. E. White, B. E. Conway and J. O. M. Bockris (Plenum Press, New York, 1996), p. 313.
- [10] F. R. A. Jorgensen, *J. Electrochem. Soc.* **117** (1970) 275.
- [11] J. Y. Welsh, *Electrochem. Technol.* **5** (1967) 504.
- [12] E. Preisler, *J. Appl. Electrochem.* **6** (1976) 301.